Traffic Asymmetry Balancing in OFDMA-TDD Cellular Networks

Ellina Foutekova, Sinan Sinanović and Harald Haas

Abstract: **This paper proposes a novel approach to interference avoidance via inter-cell relaying in cellular OFDMA-TDD (orthogonal frequency division multiple access - time division duplex) systems. The proposed scheme, termed asymmetry balancing, is targeted towards next-generation cellular wireless systems which are envisaged to have *ad hoc* and multi-hop capabilities. Asymmetry balancing resolves the detrimental base station (BS)-to-BS interference problem inherent to TDD networks by synchronizing the TDD switching points (SPs) across cells. In order to maintain the flexibility of TDD in serving the asymmetry demands of individual cells, inter-cell relaying is employed. Mobile stations (MSs) in a cell which has a shortage of uplink (UL) resources and spare downlink (DL) resources use free DL resources to off-load UL traffic to cooperating MSs in a neighboring cell using *ad hoc* communication. In an analogous fashion DL traffic can be balanced. The purpose of this paper is to introduce the asymmetry balancing concept by considering a seven-cell cluster and a single overloaded cell in the center. A mathematical model is developed to quantify the envisaged gains in using asymmetry balancing and is verified via Monte Carlo simulations. It is demonstrated that asymmetry balancing offers great flexibility in UL-DL resource allocation. In addition, results show that a spectral efficiency improvement of more than 100% can be obtained with respect to a case where the TDD SPs are adapted to the cell-specific demands.**

Index Terms: **Ad hoc, cellular, multi-hop, OFDMA, TDD.**

I. INTRODUCTION

With varying throughput, delay and traffic asymmetry requirements, the development of new solutions and concepts that allow for a flexible and dynamic radio resource allocation for the support of high peak-to-average transmission rates, and that are able to be more spectrally efficient than conventional cellular systems is a key challenge. An effective strategy which is envisioned for next-generation wireless cellular networks to ameliorate the spectral efficiency performance without increasing hardware cost is to make use of existing infrastructure and to introduce cooperation among the network entities. Naturally, such cooperation leads to multi-hop cellular networks (MCN) [1], i.e., cellular networks which have relaying capabilities. A relay station (RS) is an intermediate node between an MS and the servicing base station (BS) and the relay can be either a dedicated transceiver or an mobile station (MS). For example, in [2], Qiao, Wu, and Tonguz describe a load balancing method via mobile dedicated transceivers, which can be replaced according to user traffic demand, in order to divert traffic using the unlicensed frequency bands. However, MCNs where the relays are MSs are of special interest due the wide availability of mobile terminals, especially in highly populated areas, where network capacity becomes a limiting factor. Capacity improvement has been shown in [3] and [4], where in-cell users act as relays to form virtual antenna arrays and thereby exploit transmit diversity.

Manuscript received November 20, 2007.

The authors are with the Institute for Digital Communications at the School of Engineering & Electronics, The University of Edinburgh, Edinburgh EH9 3JL, UK, email: {E.Foutekova, S.Sinanovic, H.Haas}@ed.ac.uk.

The *ad hoc* capabilities in an MCN are actually enabled by TDD. In addition, the support for cell-independent traffic asymmetry offered by time division duplex (TDD) together with the advantages of orthogonal frequency division multiple access (OFDMA) [5], make OFDMA-TDD a promising choice for next generation wireless networks [6]. However, TDD suffers from additional interference as compared to frequency division duplex (FDD). In particular, TDD suffers from same-entity interference, MS→MS and BS→BS, which presents a major problem in actual cellular TDD deployment when cell-independent asymmetry is to be supported. Known solutions to interference avoidance in TDD include the concept of zone/region division [7], which restricts crossed slot operation only within a radius r around the BS. Optimum performance has been found for r=52% of the cell radius [7]. This strategy reduces MS→MS interference, but does not solve the more detrimental BS→BS interference problem. Moreover, it also imposes restrictions on the flexibility of TDD by compromising user demand. Furthermore, a strategy for same-entity interference mitigation, similar to frequency hopping, termed time-slot opposing, has been proposed in [8]. The time multiplexed busy tone approach in [9] also mitigates the problem of same-entity interference.

In this paper a novel idea termed *asymmetry balancing* is proposed to entirely avoid the detrimental BS→BS interference. The essence of the asymmetry balancing concept is, as the name suggests, to balance the asymmetry demand across the cells in a network. To this end, the TDD switching point (SP) is synchronized across cells, which might result in a shortage of resources in a particular cell, while a neighboring cell might have spare resources (assuming cell-independent traffic asymmetry demands). In order to resolve any mismatch between resource availability and resource demand, the *ad hoc* capabilities of an MCN are exploited. In particular, an MS which cannot be served in either uplink (UL) or downlink (DL) by its associated BS due to shortage of resources is served by a neighboring cooperating BS, which has spare resources in both link directions. The established MS↔BS link is a two-hop link where the intermediate node is an MS associated with the cooperating BS. In this way, despite the fact that the network maintains a synchronized SP, cell-specific asymmetries are effectively supported.

It is assumed that cells are differently loaded, which is a reasonable assumption for future wireless networks which will mainly support packet-data traffic characterized by a high peak-

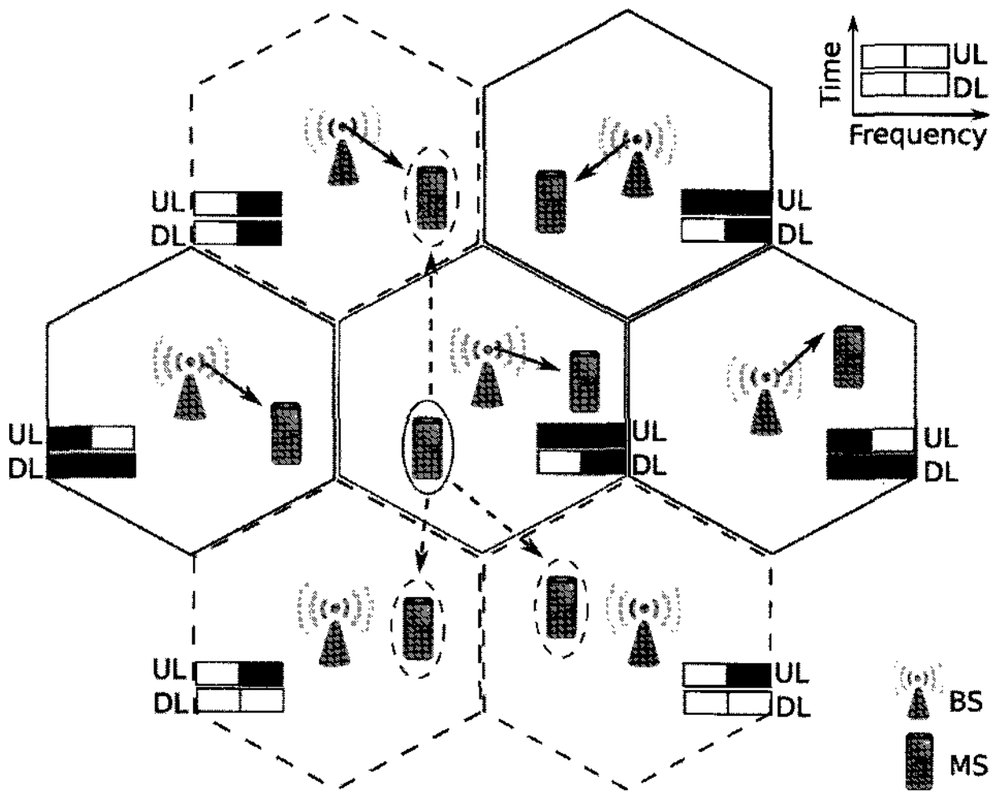

Fig. 1. The MSs in the center cell, i.e., the CoI, can off-load UL traffic to neighboring cooperating cells (marked by dashed hexagons) using free DL resources (marked by white boxes). As an example, the MS at the CoI which needs UL service (marked by a solid ellipse) can form an *ad hoc* link with any of the available MSs (marked by dashed ellipses) at the cooperating cells. Active DL links are shown as solid arrows, while possible concurrent *ad hoc* links are shown as dashed arrows.

to-average load ratio. In addition, because traffic is envisaged to be DL-favored the network-wide SP will be primarily DL-favored (or occasionally symmetric), it is expected that a cell which requires UL-favored SP will not be able to support the UL demand. Therefore, this study focuses on UL asymmetry balancing.

The rest of the paper is organized as follows. Section II introduces the novel asymmetry balancing idea and the simulation model is presented in Section III, while the results are given in Section IV. The paper concludes with Section V.

II. ASYMMETRY BALANCING VIA INTER-CELL RELAYING

As the asymmetry balancing concept relies on cooperation, it is important to identify the cooperating entities and when they can cooperate. If hexagonal cells are considered, each cell can be treated as a cell of interest (CoI), surrounded by six neighboring cells, which are the potential cooperating cells. Fig. 1 illustrates the aforementioned geometry during a DL time slot. Assume that there are only two frequency resources per cell per link direction per frame, which are marked by boxes on Fig. 1. A black box signifies an allocated resource, while a white box signifies a free resource. Let the CoI suffer from shortage of UL resources, while it has a DL resource available. Marked by a solid ellipse is the MS at the CoI, which needs UL service and desires to off-load traffic. The first-tier cells which are marked with dashed hexagons have spare UL and DL resources and hence are the cooperating cells. Associated with the cooperating cells are the MSs which can serve as RSs (identified by dashed ellipses). The tagged MS at the CoI can relay to any of the available RSs.

The MS→RS link uses a DL resource, which is free both at the CoI and the cooperating cell which serves the respective RS. Such resources are referred to as common free resources (CFR). In addition, the off-loading MSs can form *ad hoc* links to either idle MSs in neighboring cells, or active MSs which are already receiving in DL from their BS. The latter case exploits the fact that a DL transmission usually does not occupy all subchannels, and this is accounted for by the use of frequency division multiple access (FDMA) in combination with OFDM. It should be noted that in an OFDMA-TDD network the smallest resource unit allocatable to a particular user is termed a chunk[1], i.e., a number of subcarriers during one time slot.

Based on the above, the main steps of the UL asymmetry balancing technique for multiple cell scenario are summarized below:

1. A CoI is overloaded in UL and requires cooperation.
2. The set of first-tier cells surrounding the CoI, which have spare resources both in UL and DL, are the cooperating cells.
3. There are DL CFRs between the CoI and at least one of the cooperating cells.
4. Utilize the CFRs to transfer UL load from the CoI to the cooperating cells. Use *ad hoc* communication to form MS→RS links between MSs associated with the CoI and RSs associated with any of the cooperating cells.

Similarly, if the CoI suffers from DL overload, MSs at the CoI can be served indirectly by the cooperating cells via nearby MSs (operating as RSs).

From the above it can be concluded that the asymmetry balancing requires first, available resources and second, available RSs. The next two sections will treat these factors in detail. Even though the analysis is performed for the case of UL asymmetry balancing, it is valid for DL asymmetry balancing as well, by replacing UL with DL.

A. Resource Availability

When the center cell uses DL resources to off-load UL traffic to cooperating neighboring cells, UL resources are in effect created, which allow for cell-specific asymmetry demands to be supported. In this way, with cooperation the UL resource capacity of the CoI increases. For example, if the network-wide SP allocates half of the frame to UL and half to DL, and 20% of the DL resources are CFRs, the UL resource capacity of the CoI increases by 20%. Hence, an UL-to-DL traffic ratio of $\frac{0.5+0.5\times0.2}{0.5-0.5\times0.2}$, i.e., $\frac{3}{2}$, can be served at the CoI, even though the actual network-wide SP is set as $\frac{1}{1}$. This means that a "virtual" cell-specific SP can be established depending on the network-wide SP and the DL CFRs.

It is of interest to quantify the UL-to-DL ratios that a virtual SP can support, for a given network-wide SP and a given number of free resources at the CoI and its neighboring cells. Let the number of CFRs be N, where N takes on values $n \in [0, C]$, and C is the total number of resources per cell in DL. Since the SPs are synchronized across the network, C is the same for all cells. The problem of finding the distribution of N can be readily addressed by the binomial distribution, considering that having a CFR is a success, which occurs with probability p and not having such is a failure, which occurs with probability $1-p$. A success occurs when a given chunk is free at the center cell

[1]The terms chunk and resource are used interchangeably throughout this text.

and at the same time, at at least one of the neighboring cells. A failure, on the other hand, occurs when a chunk is busy at the center cell, *or* is free at the center cell and at the same time is busy at all of the neighboring cells. Thus, the distribution of the number of common free chunks, f_N, is a function of the resource occupancy probabilities at the CoI and at the first-tier cells. Resource occupancy probability is the probability that a chunk is occupied. The formulation of f_N is given in (1):

$$f_N(n) = p(L_{\mathrm{c}}, L_{\mathrm{t},1}, \cdots, L_{\mathrm{t},B_{\mathrm{t}}}, B_{\mathrm{t}})^n \cdot [1 - p(L_{\mathrm{c}}, L_{\mathrm{t},1}, \cdots, L_{\mathrm{t},B_{\mathrm{t}}}, B_{\mathrm{t}})]^{C-n} \binom{C}{n} \quad (1)$$

where B_{t} is the number of cooperating cells; $L_{\mathrm{t},i}$ is the probability that a resource is occupied at a first-tier cell i; L_{c} is the probability that a resource is occupied at the CoI; and $p(L_{\mathrm{c}}, L_{\mathrm{t},1}, \cdots, L_{\mathrm{t},B_{\mathrm{t}}}, B_{\mathrm{t}})$, which is the probability of having a CFR, depending on the number of cooperating cells and the resource occupancy, is given in (2):

$$p(L_{\mathrm{c}}, L_{\mathrm{t},1}, \cdots, L_{\mathrm{t},B_{\mathrm{t}}}, B_{\mathrm{t}}) = (1 - \prod_{i=1}^{B_{\mathrm{t}}} L_{\mathrm{t},i}) \cdot (1 - L_{\mathrm{c}}). \quad (2)$$

The expected value of the binomial distribution in (1) yields $E[N] = C \cdot p$, hence the expected value of the number of CFRs as a fraction of the total number of DL resources is $\frac{E[N]}{C} = p$.

Let the network-wide SP split the frame into two sub-frames, such that their time durations are in ratio of $u : d$, where $\frac{u}{u+d}$ of the time the frame is in UL and $\frac{d}{u+d}$ of the time the frame is in DL. Furthermore, let the total (UL+DL) number of chunks available per cell be C_{tot}. Then at the CoI, the expected value of the fraction of resources in the frame which can be used for UL traffic including off-loading, R_{ul}, is:

$$R_{\mathrm{ul}} = \frac{\frac{u}{u+d} C_{\mathrm{tot}} + p \frac{d}{u+d} C_{\mathrm{tot}}}{C_{\mathrm{tot}}} \equiv \underbrace{\frac{u}{u+d}}_{\text{actual SP}} + \underbrace{\frac{p\,d}{u+d}}_{\text{virtual SP}}. \quad (3)$$

This means that at the CoI the virtual SP divides the frame in an UL-to-DL ratio of $(u + p\,d) : (d - p\,d)$. It can be observed that when $p \to 0$, i.e., when there are no available resources for off-loading, then the resource allocation is according to the actual network-wide SP. When $p \to 1$, i.e., when all DL resources at the CoI can be used to off-load UL traffic, then $R_{\mathrm{ul}} \to 1$ and the whole frame can be allocated to UL.

Fig. 2 shows a plot of $R_{\mathrm{ul}} \times 100\%$ depending on the actual SP, the number of cooperating BSs, and on the resource occupancies at the CoI and at the cooperating BSs. In order to study the effect of the virtual SP a best-case and a worst-case scenario are considered. The number of cooperating BSs is one for the worst-case scenario and six for the best-case scenario. The resource occupancies in the case when all six cells can cooperate are kept the same ($L_{\mathrm{t},1} = L_{\mathrm{t},2} = \cdots = L_{\mathrm{t}}$), while when only one cell cooperates $L_{\mathrm{t},1} = L_{\mathrm{t},2} = \cdots = L_{\mathrm{t},5} = 1$ and $L_{\mathrm{t},6} = L_{\mathrm{t}}$. The values for L_{t} are varied as shown in Fig. 2. Overall, it can be observed that, as expected, when there are no free resources (L_{c} and/or L_{t} are one), the virtual SP is the same as the network-wide SP. Consequently, when there are free DL resources, the virtual SP exploits the resource availability to allocate additional resources to UL. Furthermore, when all DL resources at the CoI are free, the whole frame can be allocated to UL for low to moderate loads at the cooperating cells when six cells cooperate. Even in the case when only one cell cooperates the same effect can be achieved if $L_{\mathrm{t}} = 0$. As expected, when overall the DL resource occupancy increases, the number of resources allocated to UL by the virtual SP at the CoI decreases. It is interesting to note that due to the six degrees of freedom, when six cells cooperate, $R_{\mathrm{ul}} \times 100\%$ decreases much slower with decrease in resource availability as compared to the case when only one cell cooperates, where $R_{\mathrm{ul}} \times 100\%$ decreases linearly. Overall, it is seen that asymmetry balancing offers flexibility in resource allocation and can adaptively allocate resources based on availability and potentially can give all the resources in a frame to one link direction.

B. Relay Station Availability

The previous section determined the expected number of resources, which are available for off-loading and this section concentrates on the second enabler for asymmetry balancing, i.e., availability of RSs. Given that there is a CFR, the CFR can be utilized if RSs are available such that a two-hop path can be found from the MS, which needs to off-load traffic to the cooperating BS. In other words, the MS→RS *ad hoc* links are "opportunistic" in that they exploit CFRs and available RSs, and also are managed in a decentralized fashion. How to find a two-hop path is a matter of routing, and determining an optimum routing strategy is beyond the scope of the current study. It is assumed here that future wireless networks will be equipped with multi-hop and relaying functionality in which case no significant additional signaling overhead is required for managing the MS→RS links.

In this study a simple path loss based routing scheme is implemented which is illustrated with the help of Fig. 3: $\mathrm{BS_{CoI}}$ faces shortage of UL resources and $\mathrm{MS_{OL}}$ needs to relay to $\mathrm{RS_c}$, which is associated with the cooperating $\mathrm{BS_c}$. $\mathrm{RS_c}$ is chosen as an RS if two conditions, $\mathrm{C_1}$ and $\mathrm{C_2}$, are satisfied (not considering protection of on-going links):

$$\mathrm{C_1} : L_{\mathrm{p}}^{\mathrm{mb}} > L_{\mathrm{p}}^{\mathrm{mr}} + \Delta_1[\mathrm{dB}]$$
$$\mathrm{C_2} : L_{\mathrm{p}}^{\mathrm{mb}} > L_{\mathrm{p}}^{\mathrm{br}} + \Delta_2[\mathrm{dB}]$$

where $L_{\mathrm{p}}^{\mathrm{mb}}$ is the path loss between $\mathrm{BS_{CoI}}$ and $\mathrm{MS_{OL}}$; $L_{\mathrm{p}}^{\mathrm{mr}}$ is the path loss between $\mathrm{MS_{OL}}$ and $\mathrm{RS_c}$; $L_{\mathrm{p}}^{\mathrm{br}}$ is the path loss between $\mathrm{BS_c}$ and $\mathrm{RS_c}$; and Δ_1 and Δ_2 are path loss margins, which are addressed later in this text. The two conditions above aim to ensure that the two-hop link $\mathrm{MS_{OL}} \to \mathrm{RS_c} \to \mathrm{BS_c}$ would be able to achieve better link capacity than the potential single hop $\mathrm{MS_{OL}}$→$\mathrm{BS_{CoI}}$ link. $\mathrm{MS_{OL}}$ and $\mathrm{RS_c}$ attain information about $L_{\mathrm{p}}^{\mathrm{mb}}$ and $L_{\mathrm{p}}^{\mathrm{br}}$, respectively, via the pilot signals that BSs typically send. In addition, $L_{\mathrm{p}}^{\mathrm{mr}}$ can be calculated using the busy burst signaling technique described in [9] and [10]. There a receiver transmits a time-multiplexed signal upon successful transmission to reserve a resource. In this study it is assumed that a time-multiplexed signal is transmitted by all receivers, which wish to reserve a particular resource. This busy

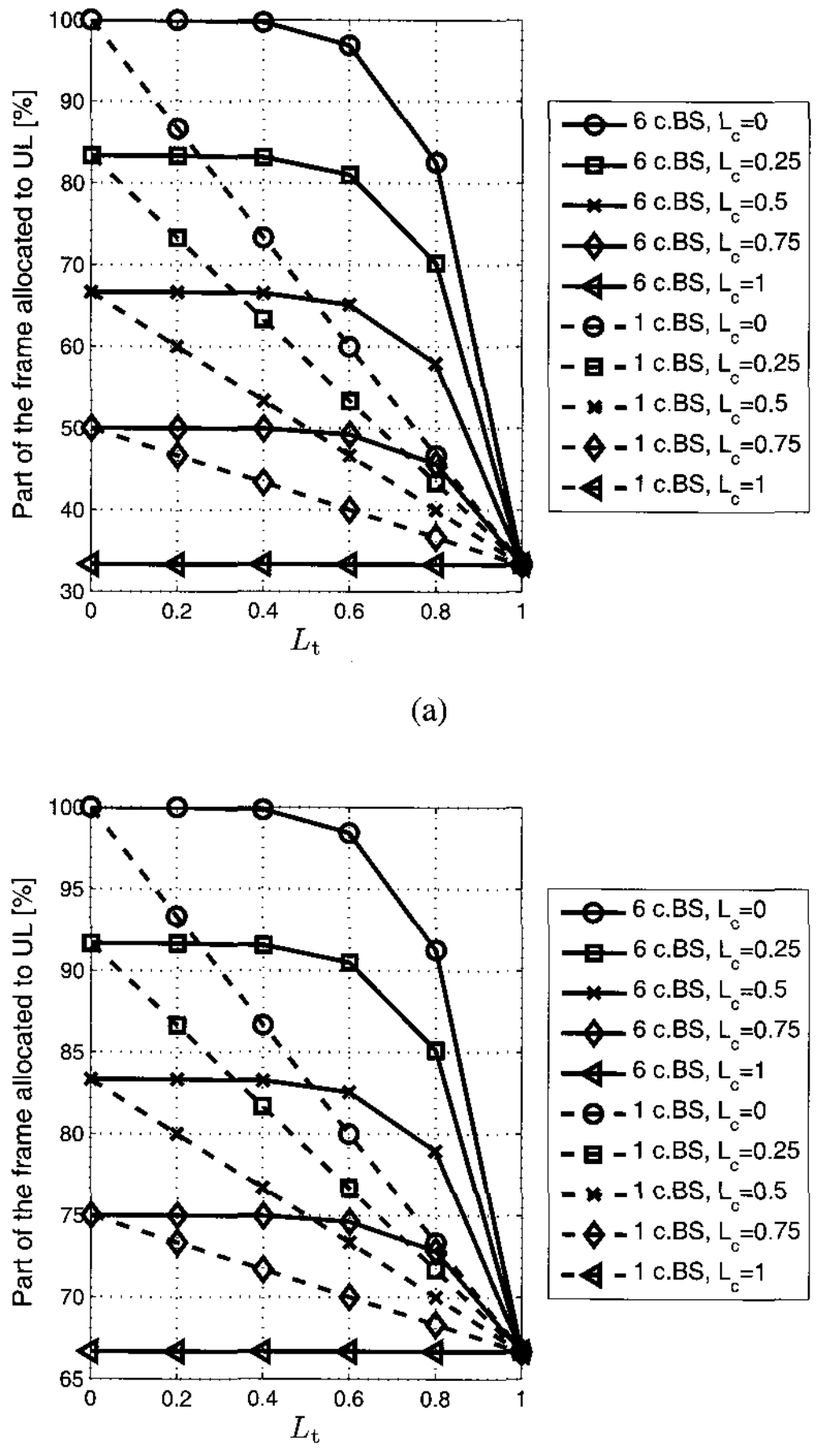

(a)

(b)

(c)

Fig. 2. The number of cooperating BSs (c.BS) takes on values of 1 and 6: (a) The network-wide SP allocates 33% of the frame to UL (base line), (b) The network-wide SP allocates 66% of the frame to UL (base line), and (c) The network-wide SP allocates 50% of the frame to UL (base line). The virtual SP can allocate additional resources to UL (up to 100% of the frame resources), based on the actual network-wide SP, as well as on the resource occupancies at the CoI and its neighboring cells.

burst signal can be used by the receiver to "advertise" its availability to serve as an RS by means of piggy-back signaling. In addition, essential information, such as $L_{\mathrm{p}}^{\mathrm{br}}$, can be readily obtained from the received busy burst signal at the $\mathrm{MS_{OL}}$ given

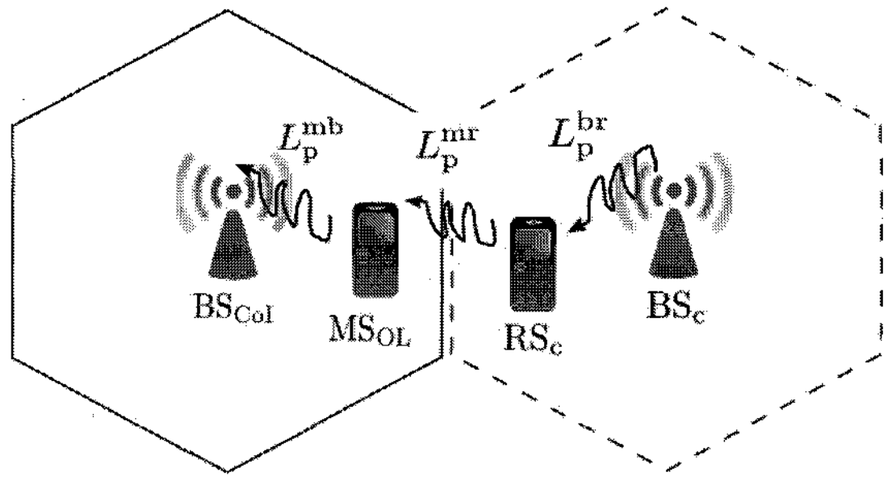

Fig. 3. $\mathrm{MS_{OL}}$ decides whether to off-load to $\mathrm{RS_c}$ or not based on a comparison of $L_{\mathrm{p}}^{\mathrm{mb}}$ with $L_{\mathrm{p}}^{\mathrm{mr}}$ and $L_{\mathrm{p}}^{\mathrm{mb}}$ with $L_{\mathrm{p}}^{\mathrm{br}}$.

that the busy burst power emitted from the RS is constant. As a consequence, $\mathrm{MS_{OL}}$ is equipped to evaluate the routing conditions quoted above in a decentralized fashion and, hence, is enabled to find a suitable RS.

Based on the above, given a CFR is shared between the CoI and a number of first-tier cells, K, the probability, p_{ucfr}, that the CFR will be utilized, is the probability that at least one user at the CoI will be able to find at least one two-hop path, which satisfies both C_1 and C_2. p_{ucfr} can be expressed as given in (4):

$$p_{\mathrm{ucfr}} = 1 - (1 - \Pr\{\mathrm{C}_1 \cap \mathrm{C}_2\})^{U_{\mathrm{c}}^2 K} \tag{4}$$

where U_{c} is the number of users per cell; and $\Pr\{\mathrm{C}_1 \cap \mathrm{C}_2\}$ is the probability that both C_1 and C_2 are satisfied at the same time and can be determined using conditional probabilities as given in (5):

$$\Pr\{\mathrm{C}_1 \cap \mathrm{C}_2\} = \Pr\{\mathrm{C}_1 \mid \mathrm{C}_2\}\Pr\{\mathrm{C}_2\} \tag{5}$$

where $\Pr\{\mathrm{C}_1 \mid \mathrm{C}_2\}$ and $\Pr\{\mathrm{C}_2\}$ are defined below:

$$\Pr\{\mathrm{C}_1 \mid \mathrm{C}_2\} = \Pr\{L_{\mathrm{p}}^{\mathrm{mr}} < L_{\mathrm{p}}^{\mathrm{mb}} - \Delta_1 \mid L_{\mathrm{p}}^{\mathrm{br}} < L_{\mathrm{p}}^{\mathrm{mb}} - \Delta_2\} \tag{6}$$

$$\Pr\{\mathrm{C}_2\} = \Pr\{L_{\mathrm{p}}^{\mathrm{br}} < L_{\mathrm{p}}^{\mathrm{mb}} - \Delta_2\}. \tag{7}$$

The path losses are random variables and their distributions can be derived by approximating the hexagonal cell structure by a circular cell structure as shown in the Appendix. In particular, both $L_{\mathrm{p}}^{\mathrm{br}}$ and $L_{\mathrm{p}}^{\mathrm{mb}}$ are BS–MS path loss distributions which are identically distributed and their probability distribution function (pdf) is approximated as follows (for the derivation please refer to the Appendix):

$$f_q(q) = \frac{2}{R^2 b} 10^{2\frac{q-a}{b}} \ln(10), \quad q \le a + b\log_{10}(z) \tag{8}$$

where R is the cell radius, a is an environment specific constant and $b = 10\,\mu$ with μ being the path loss exponent. Similarly, the MS-RS path loss distribution $L_{\mathrm{p}}^{\mathrm{mr}}$ is approximated by the following pdf (again, for the derivation please refer to the Appendix):

$$f_y(y) = \int_0^R f_y(y|z) f_z(z)\, dz \tag{9}$$

where $f_z(z)$ is the distribution of the distances [9]:

$$f_z(z) = \frac{2\,z}{R^2}, \quad z \le R \tag{10}$$

Table 1. Probability p_{ucfr} that at least one two-hop link can be established for five users per cell and $\Delta_1 = \Delta_2 = 3$ dB.

# of coop BSs:	1	2	3	4	5	6
S-A:	0.010	0.021	0.031	0.041	0.051	0.061
sim.:	0.009	0.018	0.032	0.043	0.051	0.065

and $f_y(y|z)$ is path loss distribution for a given distance from the center, z.

Based on the above, (6) can be further evaluated as follows:

$$\Pr\{L_{\mathrm{p}}^{\mathrm{mr}} < L_{\mathrm{p}}^{\mathrm{mb}} - \Delta_1 \mid L_{\mathrm{p}}^{\mathrm{br}} < L_{\mathrm{p}}^{\mathrm{mb}} - \Delta_2\} = \int_{\forall m} \int_{\forall r}^{m-\Delta_2} F_y(m-\Delta_1) f_q(r) f_q(m) \mathrm{d}m\mathrm{d}r \quad (11)$$

where m and r are dummy variables; $f_q(r)$ is given in (8); and $F_y(m)$ is the cumulative distribution function (cdf) according to the pdf in (9). The limits of the integration are determined by the cell dimensions and path loss models. In addition, (7) can be determined as :

$$\Pr\{L_{\mathrm{p}}^{\mathrm{br}} < L_{\mathrm{p}}^{\mathrm{mb}} - \Delta_2\} = \int_{\forall m} F_q(m-\Delta_2) f_q(m) \mathrm{d}m \quad (12)$$

where $F_q(m)$ is the cdf that corresponds to the pdf in (8).

In order to obtain (4), (11) and (12) are numerically evaluated. Five users per cell are used and as an example, $\Delta_1 = \Delta_2 = 3$ dB. First of all, the value for $1 - \Pr\{\mathrm{C}_1 \cap \mathrm{C}_2\}$ is obtained. According to simulation, $1 - \Pr\{\mathrm{C}_1 \cap \mathrm{C}_2\} \approx 0.99958$, while according to the approximation, $1 - \Pr\{\mathrm{C}_1 \cap \mathrm{C}_2\} \approx 0.99765$. This means that the circular geometry approximation appears to be a lower bound on the probability of not finding a suitable two-hop link. Clearly, when using these findings in the original formula for p_{ucfr} the discrepancy will increase exponentially with the power of $U_{\mathrm{c}}^2 K$. Hence, in order to verify the mathematical model presented, a semi-analytical approach is taken. Namely, the simulation result for $1 - \Pr\{\mathrm{C}_1 \cap \mathrm{C}_2\}$ is used and applied to the formula for p_{ucfr}. The model for p_{ucfr} is successfully verified by simulation and a comparison between semi-analytical and simulation results is shown in Table 1, denoted by S-A and sim., respectively. As expected, when the number of cooperating BSs increases, the probability that at least one two-hop link is found which satisfies both C_1 and C_2 increases. It is interesting to determine how many users per cell are required in order for a two-hop link to be always available, i.e., for p_{ucfr} to become one. Because the simulation result for $1 - \Pr\{\mathrm{C}_1 \cap \mathrm{C}_2\}$ is closer to one than the theoretical result, p_{ucfr} when obtained via simulation will converge slower. It can be calculated that for 110 users per cell and just one cooperating cell, p_{ucfr} is 0.994. Clearly, when more than one cooperating cell is available, convergence to one is reached faster. In fact, for all practical purposes, for more than 150 users per cell, p_{ucfr} is actually one. For a cell radius of 500 m, the cell area is 0.87 km^2, which means about 170 users per km^2. This is a reasonable number, as even suburban areas have at least 100 users per km^2 and typically in the order of thousand (depending on the wireless provider market share) [11], [12].

It is important to mention that the choice of Δ_1 and Δ_2 has a significant influence on the performance of asymmetry balancing. First of all, Δ_1 and Δ_2 influence how fast p_{ucfr} converges to one. For example, if Δ_1 is kept at 3 dB, but Δ_2 is increased to 5 dB, then according to simulation around 200 users per cell are necessary (240 users per km^2) for p_{ucfr} to become one. In addition, Δ_1 and Δ_2 control the choice of off-loading MSs and serving RSs. As an example, Fig. 4(a) shows the distribution of the off-loading MSs and the serving RSs for $\Delta_1 = \Delta_2 = 3$ dB (using the path loss models specified in Section III). It can be seen that as intended, MSs at the cell edges off-load to better-placed MSs in terms of path loss (log-normal shadowing is not considered). Furthermore, as seen when comparing Fig. 4(a) with Fig. 4(b), increasing Δ_2 for a given Δ_1 will move the "belt" of RSs closer to their associated BSs. In contrast, increasing Δ_1 for a given Δ_2 will shrink both the "belt" of RSs and the "belt" of MSs, as can be seen when comparing Fig. 4(a) with Fig. 4(c). Multi-hop link optimization strategies are presented in [13]. Because optimization of Δ_1 and Δ_2 pertains to the particular routing strategy in place, it is not considered in this study and $\Delta_1 = \Delta_2 = 3$ dB is used.

It can be seen from the above that users at the cell-edges are most likely to use two-hop links. Hence, asymmetry balancing can be combined with "smart" scheduling such that when a given BS faces overload, it gives priority to users, which are closer to the cell center, thus encouraging users which are closer to the cell edges to use two-hop communication. "Smart" scheduling for load balancing is beyond the scope of this paper.

III. SIMULATION MODEL

An OFDMA-TDD system, designed according to the UL asymmetry balancing model introduced in Section II, is simulated using a Monte Carlo approach. Each of the seven cells has a centrally-placed omnidirectional BS and full frequency reuse is assumed. Due to complexity issues only twenty users are distributed uniformly in each of the seven cells. The users are distributed at the beginning of each iteration and a snap-shot analysis is performed. For simplicity and demonstration purposes, the UL↔DL SPs are synchronized across the cells at the symmetric state. However, the model can readily be applied to any asymmetry ratio. Similarly to the envisaged traffic asymmetry in data-packet services, traffic is on average DL-favored. The center cell, however, is UL-overloaded and hence generates UL-favored traffic. The holding time is the same for all users and equals one chunk during a time slot (5 OFDM symbols). Each cell is imposed a mean offered load, which governs the respective user mean inter-arrival times and each user independently generates holding times with exponentially distributed interarrival times. The traffic per user is stored in a buffer and served on a first-in-first-out basis. Path loss is calculated using the WINNER C1 path loss model (NLOS) for urban environment [14] as shown below:

$$L_{\mathrm{p}} = a + b \log_{10}(d) \quad (13)$$

where L_{p} is the path loss in dB, a and b are given in Table 2, and d is the transmitter-receiver separation distance in meters. It should be noted that the values of a and b depend on whether MS–RS path loss, BS–MS path loss, or BS–BS path loss is

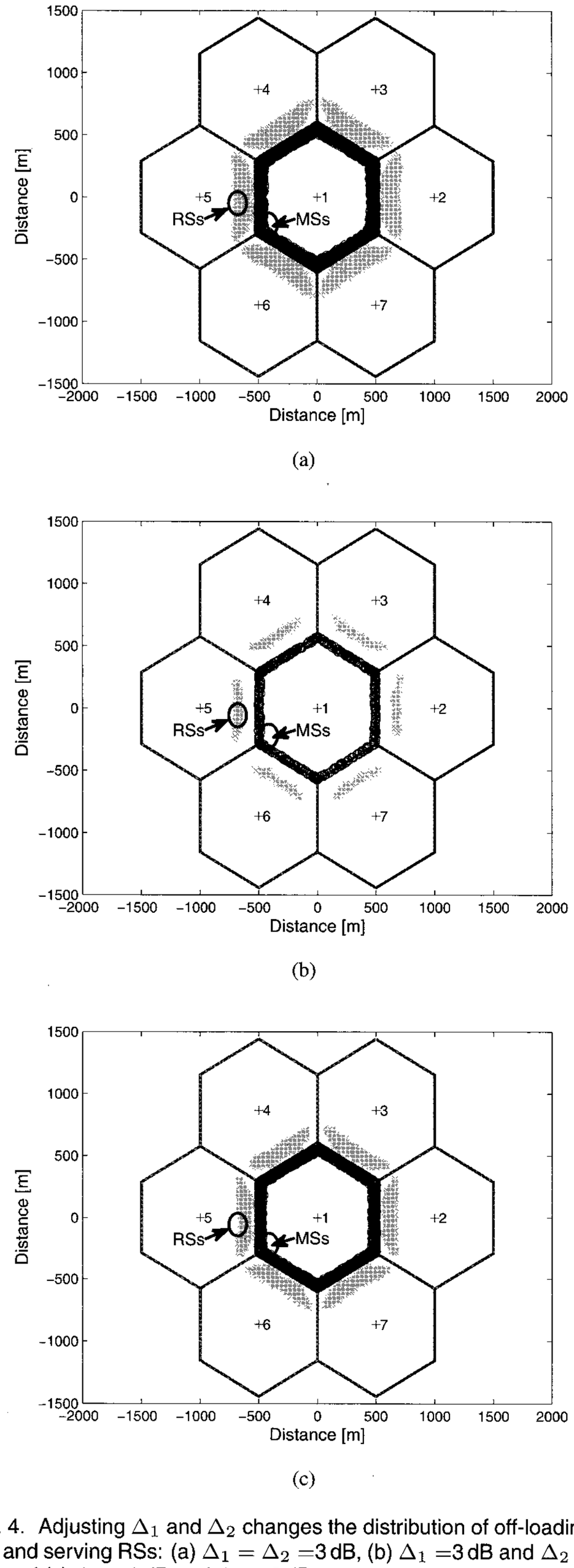

(a)

(b)

(c)

Fig. 4. Adjusting Δ_1 and Δ_2 changes the distribution of off-loading MSs and serving RSs: (a) $\Delta_1 = \Delta_2 = 3$ dB, (b) $\Delta_1 = 3$ dB and $\Delta_2 = 6$ dB, and (c) $\Delta_1 = 6$ dB and $\Delta_2 = 3$ dB.

calculated. For the latter line-of-sight conditions are assumed. MSs are associated with serving BSs based on minimum path loss. Perfect synchronization is assumed and only co-channel interference from all active other-cell transmitters is taken into account. Time-frequency resources are allocated following a score-based approach [15], where the score is evaluated based on buffer-size. In particular, a given resource is allocated to the user with the largest average buffer size, monitored during a time window of eight frames. The simulation parameters are shown in Table 2. For demonstration purposes, 16 OFDM subcarriers are considered (subject to slow fading effects only). As the SP is symmetric, both UL and DL are allocated 16 subcarriers/time slot $\times$ 3 time slots/frame = 48 chunks/frame (as one chunk is one subcarrier). The transmit power per chunk is fixed to the maximum transmit power divided by the number of chunks per time slot.

Table 2. Simulation parameters [14], [16].

Carrier frequency	5 GHz
Time slot duration	0.1152 ms
Number of time slots/ frame	6
Number of OFDM symbols/ time slot	5
Transmit power/ link	251 mW (24 dBm)
Shortest BS-BS distance	1 km
BS height	25 m
MS height	1.5 m
Path loss parameter a	MS–BS: 39.61 MS–RS: 32.49 BS–BS: 41.2
Path loss parameter b	MS–BS: 35.74 MS–RS: 43.75 BS–BS: 23.8

IV. RESULTS AND DISCUSSION

In this study, the performance of UL asymmetry balancing is investigated. Therefore, it is assumed that the UL in the CoI is overloaded and two particular scenarios in terms of resource availability are defined: (1) A best case 6-cell scenario, where all six first-tier cells cooperate; and (2) a worst-case 1-cell scenario where only one first-tier cell cooperates. (Technically, the worst case is if zero cells cooperate and will be considered later.) Different resource availability conditions are enforced by varying the total *user demand* per frame per cell (in %). In this paper, the synchronized SP is set to allocate half of the frame resources to UL and DL each. As a result, in order to obtain the *probability for resource occupancy* at a particular link direction for a given cell, the respective user demand should be multiplied by 2 (because the user demand is defined on a frame basis). The DL resource occupancy probability both at the CoI and at the cooperating cells is varied from 0 to 0.8, which corresponds to a user demand that varies from 0% to 40%. In order to account for a worst case scenario in terms of interference experienced by the *ad hoc* links, the non-cooperating cells are assumed to be fully loaded in DL (i.e., the demand is 50%). Because the UL resource demand of the first-tier cells would not influence the results for UL asymmetry balancing, it is kept constant for all considered scenarios. The UL and DL resource demands are shown in Table 3. In order to confirm the theoretic model presented in Section II, results displaying the virtual SP at the CoI for the 6-cell scenario and for the 1-cell scenario are shown in Fig. 5 and a perfect match between simulation and theory is ob-

Table 3. Resource demand for UL and DL (in %).

Cell number → Link direction ↓	1 (CoI)	2	3	4	5	6	7
UL	100	15					
DL (6-cell)	0→40						
DL (1-cell)	0→40	50					

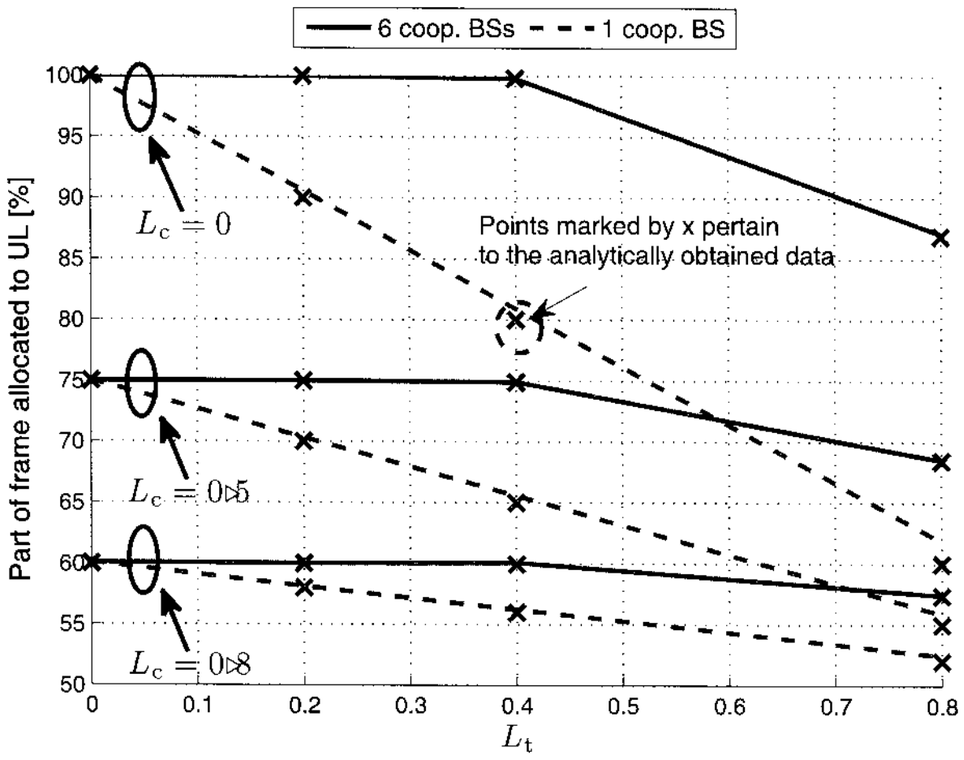

Fig. 5. Frame resources allocated to UL at the CoI by the virtual SP. Solid and dashed lines show simulation results, while analytically obtained data points are marked by "x".

served.

Next, the performance of the UL asymmetry balancing scheme is compared against two systems: 1) An independent SP (ISP) system where each cell independently sets its SP based on the ratio of UL and DL resource demands; and 2) a synchronized SP (SSP) system which is the same as the asymmetry balancing system, but off-loading does not take place. The comparison metric is spectral efficiency as given in (14), because it can capture not only user link conditions, but also how efficiently resources in a frame are utilized:

$$C_{\mathrm{b}} = \frac{1}{C_{\mathrm{tot}}} \left(\sum_{i=1}^{M} \log_2(1+\gamma_i) + \frac{\overline{M}_{\mathrm{OL}}}{M_{\mathrm{OL}}} \sum_{j=1}^{M_{\mathrm{OL}}} \log_2(1+\gamma_j^{\mathrm{mh}}) \right) \tag{14}$$

where C_{b} is the spectral efficiency per chunk in bps/Hz; γ_i is the SINR of chunk i for single hop links; $M = \frac{u}{u+d} C_{\mathrm{tot}}$ is the number of chunks allocated to UL as per the network-wide SP; $\overline{M}_{\mathrm{OL}} = p\frac{d}{u+d} C_{\mathrm{tot}}$, is the number of DL chunks available for off-loading; M_{OL} is the number of chunks actually utilized for off-loading; and γ_j^{mh} is the SINR of chunk j for two-hop links. Clearly, for systems which do not employ asymmetry balancing, $p = 0$, and the second term of the summation in (14) produces a zero. In addition, it should be noted that γ_j^{mh} is taken as the minimum of the SINR achieved at the first and second hops for each two-hop link. Furthermore, $\frac{\overline{M}_{\mathrm{OL}}}{M_{\mathrm{OL}}}$ is used as a correction factor for the following reason. Due to simulation complexity, only twenty users per cell are simulated. As a result, not all available CFRs can be utilized for off-loading via a neighboring RS. The number of available CFRs is only influenced by the

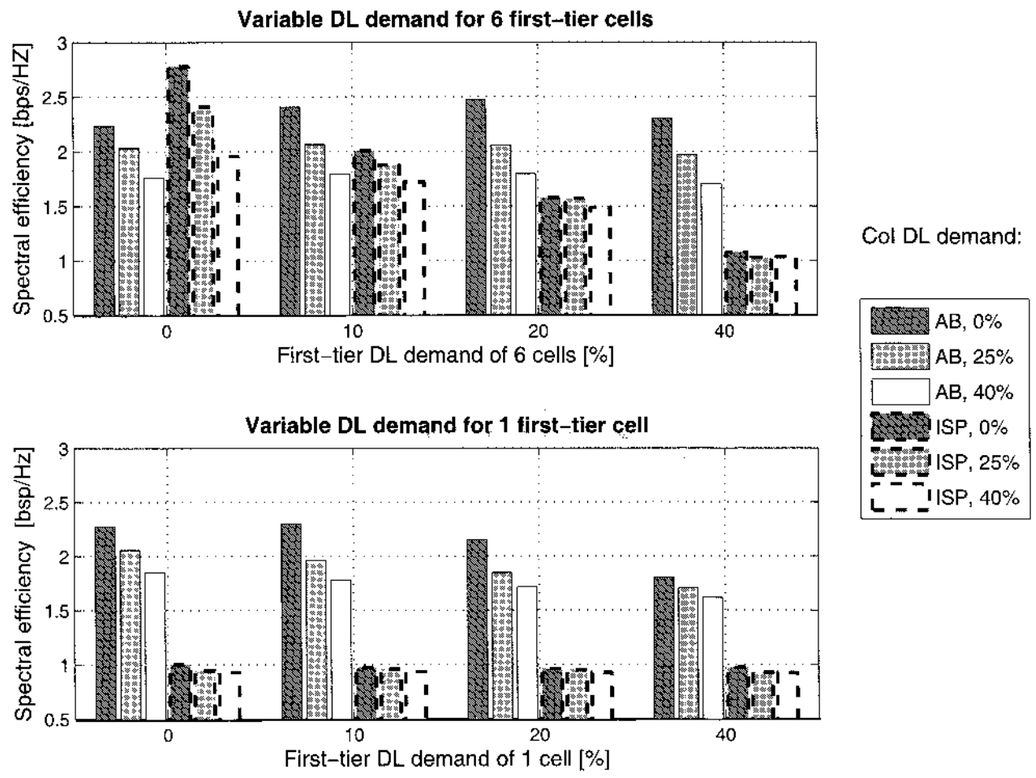

Fig. 6. UL spectral efficiency performance at the CoI achieved with asymmetry balancing (AB) as compared to an ISP system.

actual load, i.e., fraction of available resources, which is independent of the number of users in the system. In contrast, how many of the available CFRs can be utilized for MS→RS links depends on user density (active and non-active users alike) because user density determines if and how often a two-hop path can be found. As a consequence, the spectral efficiency results are also influenced by the number of users in the system. Because, as was demonstrated in Section II, it can be safely assumed that in realistic scenarios all available CFRs can be actually utilized, the correction factor aims to obtain representative spectral efficiency performance.

When the UL spectral efficiency performance of the CoI achieved by the asymmetry balancing scheme is compared to the spectral efficiency performance of an ISP system, the advantages of asymmetry balancing in avoiding BS→BS interference become evident. The results, presented in Fig. 6, show that when the DL demand at the first-tier cells is increased, which in effect increases the number of crossed slots and, hence, the BS→BS interference experienced by the CoI, the spectral efficiency at the CoI attained by the ISP system exhibits very poor performance. Using asymmetry balancing results in a tremendous improvement, and depending on the DL demand at the first-tier cells and at the CoI, a spectral efficiency increase of more than 100% can be achieved (referring to the 1-cell scenario with first-tier DL demand of 0% to 20%). For the considered scenarios, the ISP system results in better UL spectral efficiency for the CoI only when crossed slots are absent. Such is the case in the 6-cell scenario when the DL demand is 0%, i.e., none of the six first-tier cells has DL traffic, which is a highly unlikely situation. For the spectral effiency achieved by the asymmetry balancing system, there is a common trend that as the DL resource demand increases (at the CoI and first-tier cells alike), the spectral efficiency at the CoI decreases. This is as expected, because with an increase in resource demand fewer resources are used for load balancing.

Next, the spectral efficiency attained by asymmetry balancing is compared to that attained by an SSP system, where the SPs are synchronized across cells, which is a common strategy for

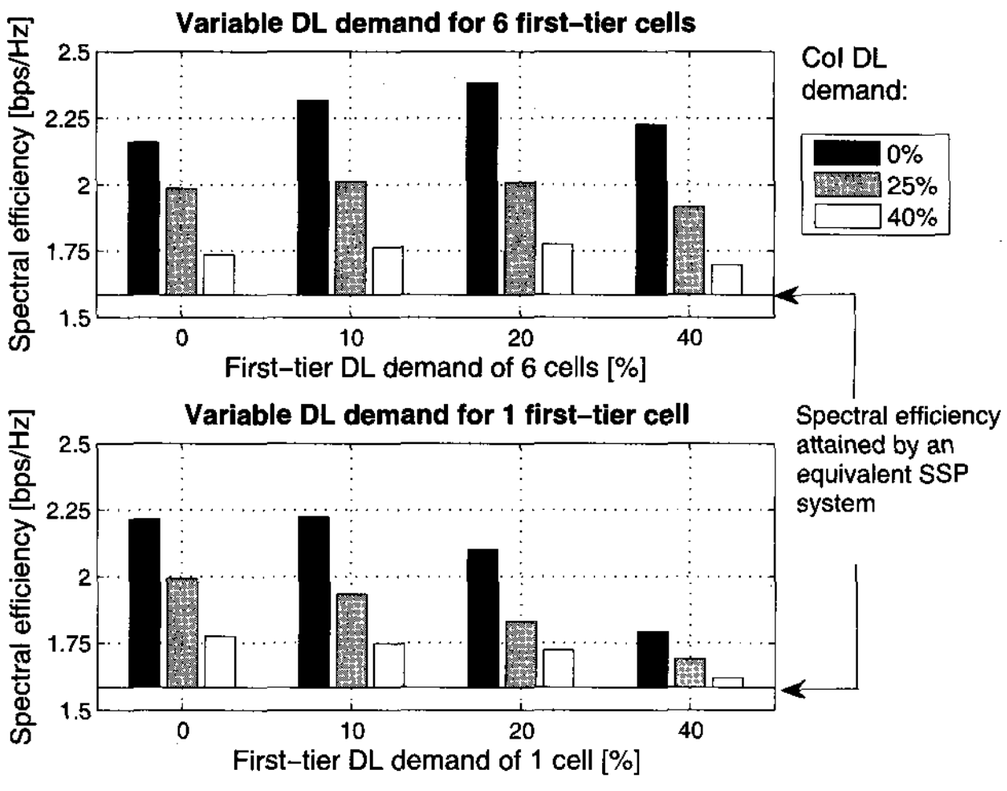

Fig. 7. Spectral efficiency performance of AB as compared to an SSP system. The spectral efficiency attained with asymmetry balancing is plotted by bars, while the spectral efficiency achieved by the SSP system is shown by a constant line as denoted on the plots.

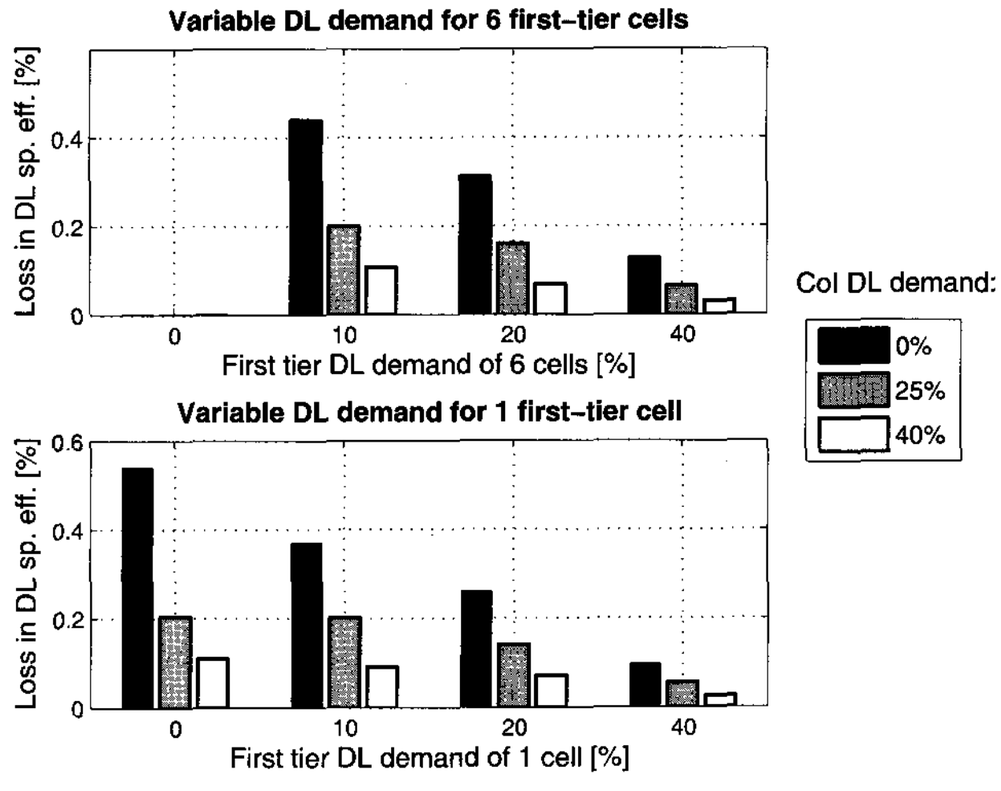

Fig. 8. Percentage loss in DL spectral efficiency caused by the off-loading *ad hoc* links as compared to an equivalent SSP system. As expected, for the 6-cell scenario at 0% DL demand at the first-tier cells, the loss is zero, because there is no DL traffic at the first-tier cells.

avoiding the detrimental BS→BS interference. Results for the UL spectral efficiency attained at the CoI with asymmetry balancing are shown in Fig. 7 for different DL demand scenarios (bar plots) and compared to the performance of an SSP system (solid line). As intuition suggests, when the SPs are synchronized, there is no difference in the CoI UL spectral efficiency performance among the considered scenarios. It is interesting to note that in tackling the poor spectral efficiency attained by the ISP system, simply synchronizing the SPs results in about 50% improvement in spectral efficiency for the cases of severe BS→BS interference (as is the 1-cell scenario), which can be seen by comparing the bottom plot of Fig. 7 and the bottom plot of Fig. 6. Employing asymmetry balancing ameliorates the spectral efficiency even further and from Fig. 7 it can be observed that the system which employs asymmetry balancing always outperforms the SSP system. In the case of 0% DL demand at the CoI, an increase in the spectral efficiency with respect to the SSP system of up to ≈50% is observed for up to 20% DL demand at the first-tier cells. When the DL demand at the CoI is increased to 25%, up to ≈25% increase in spectral efficiency is attained. In general, as expected, the more resources are allocated to UL (referring to Fig. 5), the higher the spectral efficiency achieved by asymmetry balancing. Exception to this trend is the case of 0% DL demand at the CoI (i.e., 100% of the frame resources are allocated to UL) for the 6-cell scenario (and a little less pronounced for the 1-cell scenario), where the achieved spectral efficiency increases slightly with increase in the first-tier DL demand and then decreases again. This effect is caused by using fixed transmit power per chunk. When the transmit power is fixed, the SINR decreases with an increase in the number of simultaneously active users using the same resource.

The demonstrated UL spectral efficiency amelioration attained by asymmetry balancing is at a slight loss in spectral efficiency for the first-tier DL transmission as compared to an SSP system. The loss is due to the off-loading *ad hoc* links, which generate MS→MS interference to the concurrent BS→MS links. The results presented in Fig. 8 show that overall the loss in spectral efficiency does not surpass 0.6%. It can be observed, that even though the results for the 1-cell scenario and the 6-cell scenario are similar, the loss in the case of six cooperating cells is slightly larger due to the fact that more resources are used for the off-loading *ad hoc* links and, hence, more interference is caused to the first-tier DL transmission. Furthermore, the caused loss decreases with increase in the DL demand (both at the CoI and first-tier cells), as expected, because less resources are used for off-loading. It should be noted that the spectral efficiency loss obtained for twenty users per cell is representative even for larger number of users for the studied scenarios, because the number of active users at any given time slot using any given chunk does not change and is equal to the number of cells under consideration.

Table 4. Resource demand for UL and DL (in %).

Cell number → / Link direction ↓	1 (CoI)	2	3	4	5	6	7
UL	15 90	90	75	60	45	30	15
DL	85 10	10	25	40	55	70	85

In order to complete the analysis of the asymmetry balancing scheme, it is important to consider what happens when there are no available resources for off-loading. To this end, a fully loaded system is studied (i.e., the total UL and DL demands add up to 100% for each cell), where each cell has a different traffic asymmetry demand, as shown in Table 4. For the CoI two scenarios are defined – UL-favored and DL-favored. The first-tier cells all have different asymmetry demands, which range from highly UL-favored to highly DL-favored in order to explore the crossed-slots effects on the CoI. On average three of the first-tier cells require an UL-favored SP, while the other three require a DL-favored SP. Two systems are compared, *viz:* an SSP sys-

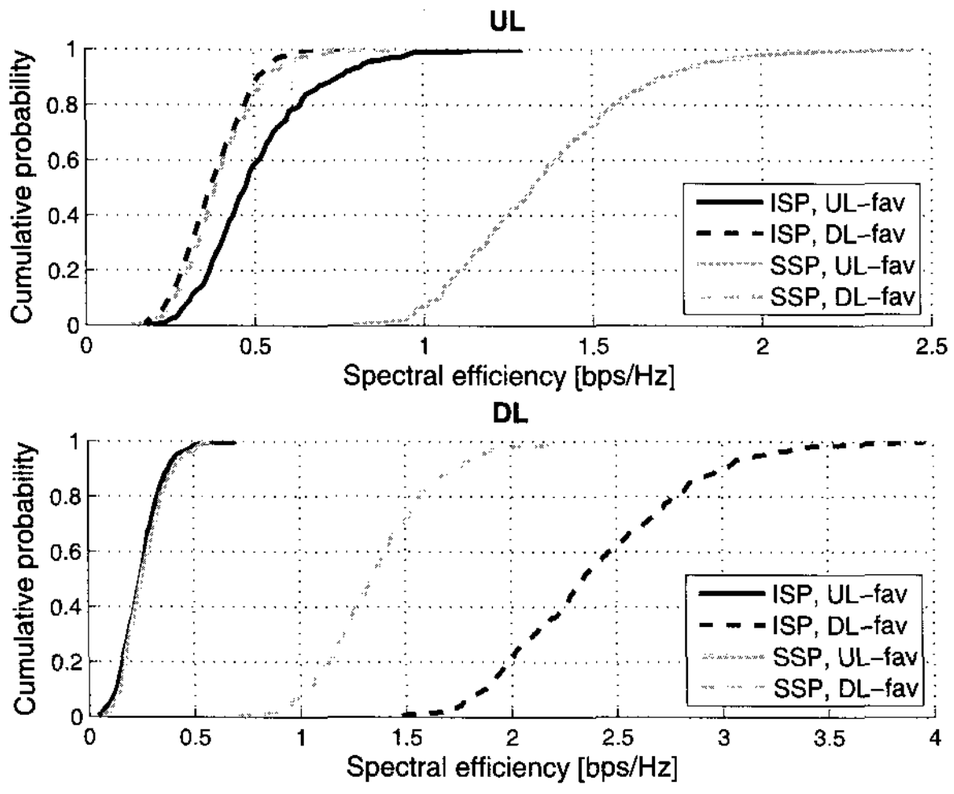

Fig. 9. Spectral efficiency comparison of an ISP system with an SSP system, under the assumption of a fully loaded network.

tem, as the asymmetry balancing system becomes an SSP system in the situation of full network load; and an ISP system. Results for the UL and DL spectral efficiency at the CoI are presented in Fig. 9 (top plot and bottom plot, respectively). When UL spectral efficiency is considered (top plot), it is observed that when the demand at the CoI is UL-favored and crossed slots are present, by avoiding crossed slots the SSP system actually achieves about 2.5 times better spectral efficiency at the 50^{th} percentile than the ISP system. As expected, when the demand at the CoI is DL-favored, the UL spectral efficiency at the CoI is the same for an ISP system and an SSP system. Similarly, when considering the DL spectral efficiency at the CoI (bottom plot), for low DL demand, the ISP system and the SSP system attain similar performance. However, when the DL demand at the CoI is increased, the ISP system manages to provide about 1.7 times better spectral efficiency at the 50^{th} percentile than the SSP system. Here it is important to point out that MS→MS interference is not expected to be a detrimental problem in OFDMA-TDD systems because in order to have high MS→MS interference two MSs need to be using the same chunks at the same time in very close proximity to each other. The situation is different in the case of BS→BS interference, as BS positions are fixed and the whole bandwidth is reused in each cell.

It can be summarized that overall the results demonstrate that allowing each cell to set its SP independently leads to suboptimum results in the majority of cases, while synchronizing the SP across cells improves spectral efficiency performance significantly. Employing asymmetry balancing, i.e., keeping a network-wide SP and making use of inter-cell relaying, ameliorates the attained spectral efficiency even further. It is expected that optimizing the routing strategy will result in even better system performance.

V. CONCLUSIONS

In this paper, a method named *asymmetry balancing* has been proposed. It allows the support of cell-independent asymmetries in OFDMA-TDD next generation networks with complete avoidance of the detrimental BS→BS interference. The key to solving this issue is user cooperation in combination with inter-cell relaying. A general mathematical framework for the assessment of the proposed technique has been developed, and it has been applied to an UL study. It has been demonstrated that in the case of shortage of UL resources a virtual cell-specific SP can be established, depending on the system UL-to-DL asymmetry ratio and the available DL resources at the CoI and its six neighboring cells. When one or more cells can cooperate, even the whole frame can be virtually allocated for UL traffic. This flexibility in resource allocation comes at a relatively insignificant cost of less than 0.6% loss in DL spectral efficiency incurred due to interference caused by the *ad hoc* links. Furthermore, it is found that the asymmetry balancing technique significantly outperforms conventional approaches where the TDD SPs are synchronized cell-wide and where the TDD SPs are adapted to the cell-specific asymmetry demands. For the UL spectral efficiency of the CoI, the gains with respect to the case of fixed SPs are up to about 50%, whereas the gains with respect to the case of cell-specific SPs surpass 100%. As expected, BS→BS interference avoidance leads to tremendous spectral efficiency improvement. In addition, it has been demonstrated that when the system is fully loaded, the loss from allowing BS→BS interference can be bigger than the loss which results from not meeting DL demand by synchronizing the TDD SP cell-wide. Future work will focus on DL asymmetry balancing and the effect of power control on the *ad hoc* links as well as on the direct links.

APPENDIX

In order to determine the BS–MS and MS–RS path loss distributions the cell geometry is approximated by circular geometry (Fig. 10). The CoI is a circle with radius R and the RSs are outside this circle and within a circle with radius $3R$ (due to the hexagonal cell geometry).

Referring to the small circle, the BS–MS path loss distribution can be approximated using the distribution of the distances between the center of the circle and any point inside the circle as shown in [17]. In summary, assuming uniformly distributed points along the horizontal and vertical axes, this distribution of the distances is given in (15) [9].

$$f_z(z) = \frac{2z}{R^2}, \quad z \leq R. \tag{15}$$

The respective path loss, Q is of the form: $Q = a + b\log_{10}(Z)$, hence using variable transformation, the pdf of Q can be obtained as:

$$f_q(q) = \frac{2}{R^2 b} 10^{2\frac{q-a}{b}} \ln(10), \quad q \leq a + b\log_{10}(z). \tag{16}$$

Next, in order to determine the MS–RS path loss distribution, the problem can be formulated as finding the distribution of the distances between any point in the small circle to any point in the ring. Then, variable transformation can be used to find the distribution of the path losses.

Given that a transmitter is z [m] from the circle center, the pdf,

$f_x(x|z)$, of the MS-RS separation distances, X, can be found as:

$$f_x(x|z) = \begin{cases} \frac{1}{\pi 4R^2}\left(\pi - \arccos(\frac{z^2+x^2-R^2}{2zx})\right)x, \\ \qquad\qquad \text{for } R-z \le x < R+z \\ \frac{x}{4R^2} \\ \qquad\qquad \text{for } R+z \le x \le 3R-z \\ \frac{1}{\pi 4R^2}\arccos(\frac{z^2+x^2-(3R)^2}{2zx})x \\ \qquad\qquad \text{for } 3R-z < x \le 3R+z \end{cases} \tag{17}$$

The next step is to convert the MS–RS distance distribution to path loss distribution. The path loss model used is of the form $Y = a + b\log_{10}(X)$, hence $X = 10^{\frac{Y-a}{b}}$. The path loss distribution for a given distance from the center, z, can be obtained as:

$$f_y(y|z) = f_x(x(y)|z)\left|\frac{\mathrm{d}x(y)}{\mathrm{d}y}\right|$$

$$= \begin{cases} f_{x,1} = \frac{D}{\pi 4R^2}\left(\pi - \arccos(\frac{z^2+10^{2\frac{y-a}{b}}-R^2}{2z10^{\frac{y-a}{b}}})\right)10^{\frac{y-a}{b}} \\ \qquad\qquad \text{for } R-z \le 10^{\frac{y-a}{b}} < R+z \\ f_{x,2} = \frac{D\cdot 10^{\frac{y-a}{b}}}{4R^2} \\ \qquad\qquad \text{for } R+z \le 10^{\frac{y-a}{b}} \le 3R-z \\ f_{x,3} = \frac{D}{\pi 4R^2}\arccos(\frac{z^2+10^{2\frac{y-a}{b}}-(3R)^2}{2z10^{\frac{y-a}{b}}})10^{\frac{y-a}{b}} \\ \qquad\qquad \text{for } 3R-z < 10^{\frac{y-a}{b}} \le 3R+z \end{cases} \tag{18}$$

where $D = \frac{1}{b}10^{\frac{y-a}{b}}\ln(10)$.

Using (15), $f_y(y)$ can be obtained as (function arguments omitted for clarity):

$$f_y(y) = \int_0^R f_y(y|z)f_z(z)\,dz$$

$$= \begin{cases} \int_{R-x}^{R} f_{x,1}f_z\,dz,\ x \in [0,R]+ \\ \int_{x-R}^{R} f_{x,1}f_z\,dz,\ x \in [R,2R] \\ \int_{0}^{x-R} f_{x,2}f_z\,dz,\ x \in [R,2R]+ \\ \int_{0}^{3R-x} f_{x,2}f_z\,dz,\ x \in [2R,3R] \\ \int_{3R-x}^{R} f_{x,3}f_z\,dz,\ x \in [2R,3R]+ \\ \int_{x-3R}^{R} f_{x,3}f_z\,dz,\ x \in [3R,4R]. \end{cases} \tag{19}$$

The above equations are evaluated numerically and compared to a simple Monte Carlo simulation for verification. The results are shown in Fig. 11. The following simulation parameters (WINNER [14]) are used: R is 500 m, a is 32.49 dB and b is 43.75 dB. In the system model in this study, hexagonal cells are used. Thus, in order to verify that the circular geometry is a good approximation to the hexagonal geometry, simulation results for the path loss distribution in the case of hexagonal geometry are provided for comparison.

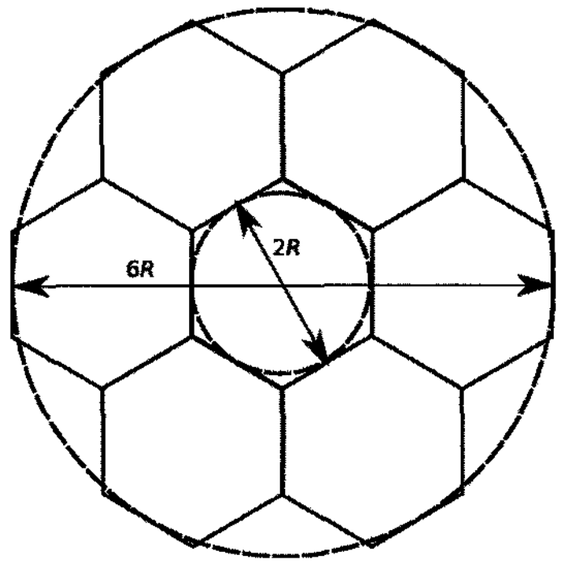

Fig. 10. Hexagonal cell geometry, approximated by circular geometry.

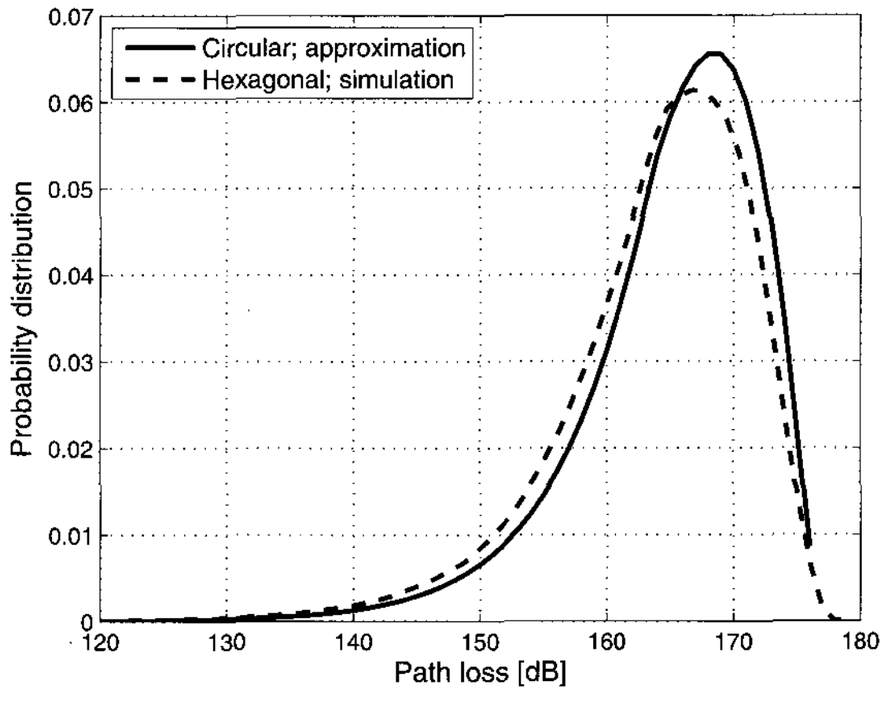

Fig. 11. Pdf of the MS–RS path losses.

ACKNOWLEDGMENT

The authors would like to thank the anonymous reviewers for their constructive and valuable comments and suggestions. The comments clearly helped to improve the manuscript.

REFERENCES

[1] L. Le and E. Hossain, "Multihop cellular networks: potential gains, research challenges, and a resource allocation framework," *IEEE Commun. Mag.*, vol. 45, no. 9, pp. 66–73, sept. 2007.

[2] C. Qiao, H. Wu, and O. Tonguz, "Load balancing via relay in next generation wireless systems," in *First Annual Workshop on Mobile and Ad Hoc Networking and Computing (MobiHOC)*, Boston, Massachusetts, USA, 11 2000, pp. 149–150.

[3] A. Sendonaris, E. Erkip, and B. Aazhang, "Increasing uplink capacity via user cooperation diversity," in *Proc. of the IEEE International Symposium on Information Theory*, Cambridge, MA, USA, 16–21 1998, p. 156.

[4] S. Yatawatta and A. Petropulu, "A multiuser OFDM system with user cooperation," in *Conference Record of the Thirty-Eighth Asilomar Conference on Signals, Systems and Computers*, vol. 1, 7–10 2004, pp. 319–323.

[5] C. Y. Wong, R. S. Cheng, K. B. Lataief, and R. D. Murch, "Multiuser OFDM with adaptive subcarrier, bit, and power allocation," *IEEE J. Sel. Areas Commun.*, vol. 17, no. 10, pp. 1747–1758, 1999.

[6] H. Haas and S. McLaughlin, Eds., *Next generation mobile access technologies: Implementing TDD*. Cambridge University Press, ISBN: 13:9780521826228, 2008, 420 pages.

[7] S.-H. Wie and D.-H. Cho, "Time slot allocation scheme based on a region division in CDMA/TDD Systems," in *Proc. of the 53rd IEEE Vehicular Technology Conference (VTC)*, Rhodes, Greece, 6–9 2001, pp. 2445–2449.

[8] H. Haas and S. McLaughlin, "A dynamic channel assignment algorithm for a hybrid TDMA/CDMA-TDD interface using the novel TS-opposing technique," *IEEE J. Sel. Areas Commun.*, vol. 19, no. 10, pp. 1831–1846, 2001.

[9] P. Omiyi, H. Haas, and G. Auer, "Analysis of TDD cellular interference mitigation using busy-bursts," *IEEE Trans. Wireless Commun.*, vol. 6, no. 7, pp. 2721–2731, 2007.

[10] G. Auer, H. Haas, and P. Omiyi, "Interference aware medium access for dynamic spectrum sharing," in *Proceedings of the 2nd IEEE International Symposium on New Frontiers in Dynamic Spectrum Access Networks (DySPAN)*, Dublin, Ireland, 17–20 2007, pp. 399–402.

[11] F. Gessler, "Developing technical standards – Balancing history and preconceptions," in *Proc. of the International Association for Management Technology Conference (IAMOT)*, Lausanne, Switzerland, Mar. 19–22 2001, p. 076FG.

[12] WiMAX Forum, "WiMAX Business Case," Available at http://www.hkwtia.org/wtia/ (Date of access: Apr. 8, 2008), 2004.

[13] J. Cho and Z. Haas, "On the throughput enhancement of the downstream channel in cellular radio networks through multihop relaying," *IEEE J. Sel. Areas Commun.*, vol. 22, no. 7, pp. 1206–1219, 2004.

[14] IST-4-027756 WINNER II, "D1.1.2 v1.2 WINNER II channel models," Retrieved Feb. 5, 2008, from https://www.ist-winner.org/WINNER2-Deliverables/.

[15] T. Bonald, "A score-based opportunistic scheduler for fading radio channels," in *Proc. of the 5th European Wireless Conference (EWC)*, Barcelona, Spain, 24–27, 2004.

[16] IST-2003-507581 WINNER, "D2.10, Final report on identified RI key technologies, system concept and their assessment," Retrieved Mar. 15, 2007, from https://www.ist-winner.org/DeliverableDocuments/, 2005.

[17] Z. Bharucha and H. Haas, "The distribution of path losses for uniformly distributed nodes in a Circle," *Research Letters in Communications*, vol. 2008, no. Article ID 376895, p. 4 pages, 2008.

Ellina Foutekova obtained her B.Sc. degree from Jacobs University Bremen, Bremen, Germany (formerly International University Bremen) in 2005. In the next year she began her Ph.D. studies at the same university and in 2007 transferred to the University of Edinburgh (UoE), Edinburgh, UK. She is currently a Ph.D. student at the Institute for Digital Communications (IDCOM) at UoE, supervised by Dr. Harald Haas. Her main research interests are in the areas of wireless communications, particularly focusing on interference avoidance, load balancing, resource allocation.

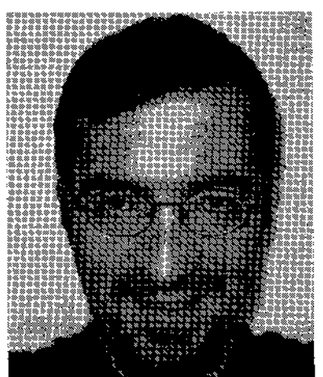

Sinan Sinanović obtained his Ph.D. in electrical and computer engineering from Rice University, Houston, Texas in 2006. In the same year, he has joined Jacobs University Bremen in Germany as a post doctoral fellow. In 2007, he has joined the University of Edinburgh in the UK where he currently works as a research fellow in the Institute for Digital Communications. He has previously worked for Texas Instruments in Dallas, Texas on ASIC for the central office modem. While working for Halliburton Energy Services in Houston, Texas, he developed acoustic telemetry receiver for which he was awarded US patent (# 7158446). He is a member of the Tau Beta Pi engineering honor society and a member of Eta Kappa Nu electrical engineering Honor society. He earned his M.S. from Rice University and his B.S.E.E. (summa cum laude) from Lamar University in Texas.

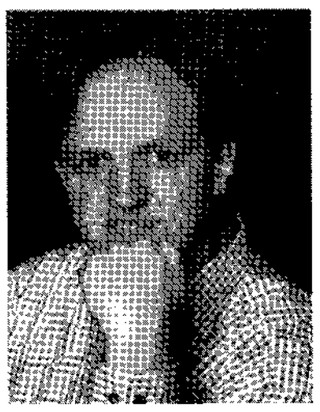

Harald Haas received the Ph.D. degree from the University of Edinburgh in 2001. His main research interests are in the areas of wireless system engineering and digital signal processing, with a particular focus on interference aware MAC protocols, multiuser access, link adaptation, scheduling, dynamic resource allocation, multiple antenna systems and optical wireless communication. From 2001 to 2002, He was project manager at Siemens AG (Information and Communication Mobile Networks) for an international research project on new radio access technologies. He joined International University Bremen (Germany), now Jacobs University Bremen, in September 2002 where he has since been associate professor of Electrical Engineering. In June 2007, He joined the University of Edinburgh (Scotland/UK) where he is Reader in the Institute for Digital Communications (IDCOM). He received a best paper award at the International Symposium on Personal, Indoor and Mobile Radio Communications (PIMRC) in Osaka/Japan in 1999 and holds more than ten patents in the area of wireless communications. He contributed a chapter to the "Handbook of Information Security" entitled "Air Interface Requirements for Mobile Data Services" by John Wiley & Sons, Inc. He co-authors a book entitled "Next Generation Mobile Access Technologies: Implementing TDD" with Cambridge University Press. His work on optical wireless communication was selected for publication in "100 Produkte der Zukunft (100 Products of the Future)" authored by Nobel Laureate T. W. Hänsch.